

Shell model results for nuclear β^- -decay properties of sd-shell nuclei

Anil Kumar¹, Praveen C. Srivastava^{1,*}, and Toshio Suzuki^{2,3}

Received October 22, 2019; Revised January 8, 2020; Accepted January 29, 2020; Published March 18, 2020

We evaluate the allowed β^- -decay properties of nuclei with Z=8–15 systematically under the framework of the nuclear shell model using the valence space Hamiltonians derived from modern ab initio methods, such as in-medium similarity renormalization group and coupled-cluster theory. For comparison we also show results obtained with fitted interaction derived from chiral effective field theory and phenomenological universal sd-shell Hamiltonian version B interaction. We have performed calculations for $O \to F$, $F \to Ne$, $Ne \to Na$, $Na \to Mg$, $Mg \to Al$, $Al \to Si$, $Si \to P$, and $P \to S$ transitions. Theoretical results for B(GT), $\log ft$ values, and half-lives are discussed and compared with the available experimental data.

Subject Index D11

1. Introduction

Due to the recent progress in nuclear theory with the development of modern effective nucleon-nucleon interactions for sd-shell nuclei, it is now possible to predict nuclear observables with appropriate accuracy. There is now much experimental data available for half-lives, $\log ft$ values, Gamow-Teller (GT) strengths, Q values, and branching fractions [1–3]. Thus it is highly desirable to study β^- -decay properties using these newly developed interactions. These theoretical and experimental developments also make it possible to evaluate the quenching factor of the effective axial-vector coupling strength g_A for single beta-decays.

The Gamow–Teller beta-decay transitions of sd-shell nuclei with five or more excess neutrons were predicted by Wildenthal et al. in Ref. [4]. A more comprehensive study of the β -decay properties of sd-shell nuclei for A=17–39 was reported by Brown and Wildenthal in Ref. [5]. In the middle of the sd shell (A=28) the effective matrix elements are quenched by an overall factor of 0.76 ± 0.03 , while an average quenching factor of 0.897 ± 0.035 was obtained by Wilkinson [6] in a similar analysis for the mass region A=6–21. The Gamow–Teller beta-decay rates for $A\leq18$ nuclei were reported in Ref. [7]. In this work the effective Gamow–Teller operators are deduced for the 0p shell from a least-squares fit to 16 experimental matrix elements. In recent years, shell model calculations for β^- -decay properties of neutron-rich Z=9–13 nuclei with $N\geq18$ were reported by Li and Ren in Ref. [8]. The importance of chiral two-body currents in nuclei for the quenching of the Gamow–Teller transitions and neutrinoless double-beta decay was reported for a Fermi-gas model in Ref. [9]. Theoretical calculations for half-lives of medium-mass and heavy neutron-rich nuclei

¹Department of Physics, Indian Institute of Technology Roorkee, Roorkee 247 667, India

²Department of Physics, College of Humanities and Science, Nihon Univerity, Sakurajosui 3, Setagaya-ku, Tokyo 156-8550, Japan

³National Astronomical Observatory of Japan, Osawa 2, Mitaka, Tokyo 181-8588, Japan

^{*}E-mail: praveen.srivastava@ph.iitr.ac.in

from quasiparticle random phase approximation based on the Hartree–Fock–Bogoliubov theory or other global models are available in the literature [10–15].

The study of nuclei towards drip lines are of great interest and many studies on these nuclei have been undertaken. After more than 20 years, the exact location of the drip line for F and Ne were recently confirmed in a RIKEN experiment [16]. In this region the ground state of several nuclei were recently confirmed, and more excited states were populated. The study of the "island of inversion" region has attracted much attention from recent radioactive ion beam facilities. The intruder configuration is important for such nuclei for, e.g., $^{28-31}$ Ne, 30,31 Na, $^{31-34,36}$ Mg, and 33 Al isotopes. The beta-decay half-lives of these nuclei become larger because of the influence of the intruder configuration in these nuclei. Due to strong deformation the wave functions of parent and daughter nuclei become different, thus reducing the B(GT) values.

In recent years ab initio approaches have been most successful in predicting nuclear structure properties of unstable nuclei. Thus it is worthwhile studying β^- -decay properties using these ab initio approaches. In the present work, our aim is to study the β^- -decay properties of Z=8-15 nuclei corresponding to earlier and new experimental data within the framework of the nuclear shell model using modern ab initio interactions. Our purpose is to study how well the recent ab initio and newly developed shell model interactions based on chiral interactions can describe the β -decay properties in the sd-shell, and also to find how much quenching is necessary for these interactions by comparing with much more experimental data than in Ref. [17]. Effective values of g_A for the sd-model space corresponding to ab initio interactions will be extracted. This work will add more information to earlier works [4–8], where shell model results with phenomenological effective interactions were reported. Since the study of β -decay properties based on ab initio methods is very limited, this is the first comprehensive study of β -decay properties in the sd-shell using ab initio interactions. The ab initio calculations of GT strengths in the sd-shell region for 13 different nuclear transitions, including electron-capture reaction rates for 23 Na(e^- , v) 23 Ne and 25 Mg(e^- , v) 25 Na were reported in Ref. [17].

This paper is organized as follows. In Sect. 2 we present details of ab initio interactions and the formalism for the β^- -decay properties. In Sect. 3 we present the theoretical results along with the experimental data. Finally, a summary and conclusions are presented in Sect. 4.

2. Theoretical formalism

2.1. Ab initio Hamiltonians

To calculate GT, $\log ft$ values, and half-lives for the sd-shell nuclei, we have performed shell model calculations using two ab initio interactions: in-medium similarity renormalization group (IM-SRG) [18,19] and coupled-cluster effective interactions (CCEI) [20,21]. We have also performed calculations with a newly fitted interaction derived from chiral effective field theory [22]. For comparison, we have also performed calculations with the phenomenological universal sd-shell Hamiltonian version B (USDB) effective interaction [23]. For the diagonalization of matrices we used the J-scheme shell model code NuShellX [24]. For the ab initio and USDB interactions, we performed the calculations in the sd-model space.

USDB starts from single-particle energies and two-body matrix elements, where the effects of three-nucleon interactions are considered to be included implicitly. The ab initio interaction, on the other hand, starts from chiral two-nucleon and three-nucleon interactions, and one-body and two-body terms outside a core are constructed. The effects of the three-nucleon forces are thus more properly treated in the ab initio approach compared with the phenomenological one.

Glazek and Wilson [25] and Wegner [26] developed techniques to diagonalize many-body Hamiltonians in free space known as the similarity renormalization group (SRG). The SRG consists of a continuous unitary transformation, parametrized by the flow parameter s, and splits the Hamiltonian H(s) into diagonal and off-diagonal parts,

$$H(s) = U^{\dagger}(s)H(0)U(s) = H^{d}(s) + H^{od}(s),$$
 (1)

where H(s = 0) is the initial Hamiltonian. Taking the derivative of the Hamiltonian with respect to s, one gets

$$\frac{dH(s)}{ds} = [\eta(s), H(s)],\tag{2}$$

where

$$\eta(s) = \frac{dU(s)}{ds}U^{\dagger}(s) = -\eta^{\dagger}(s) \tag{3}$$

is the anti-Hermitian generator of the unitary transformation. For an appropriate value of $\eta(s)$, the off-diagonal part of the Hamiltonian, $H^{\text{od}}(s)$, becomes zero as $s \to \infty$. Instead of the free space evolution, in-medium SRG (IM-SRG) has the attractive feature that one can involve 3-,..., A-body operators using only the two-body mechanism. The starting Hamiltonian H with respect to a finite-density reference state $|\Phi_0\rangle$ is given as

$$H = E_0 + \sum_{ij} f_{ij} \{a_i^{\dagger} a_j\} + \frac{1}{2!^2} \sum_{ijkl} \Gamma_{ijkl} \{a_i^{\dagger} a_j^{\dagger} a_l a_k\}$$

$$+ \frac{1}{3!^2} \sum_{ijklmn} W_{ijklmn} \{a_i^{\dagger} a_j^{\dagger} a_k^{\dagger} a_n a_m a_l\}.$$
(4)

Here, the normal-ordered strings of creation and annihilation operators obey $\langle \Phi | \{a_i^{\dagger} \cdots a_j\} | \Phi \rangle = 0$, and the E_0 , f_{ij} , Γ_{ijkl} , and W_{ijklmn} are the normal-ordered zero-, one-, two-, and three-body terms, respectively (see Refs. [27–30] for full details). In the case of IM-SRG, targeted normal ordering with respect to the nearest closed shell rather than $^{16}{\rm O}$ is adopted to take into account the three-nucleon interaction among the valence nucleons.

We use another ab initio approach to study β^- -decay properties of nuclei in the sd-shell region: CCEI. For this effective interaction, the intrinsic A-dependent Hamiltonian is given (for IM-SRG interactions also) as

$$\hat{H}_{A} = \sum_{i < j} \left(\frac{(\mathbf{p}_{i} - \mathbf{p}_{j})^{2}}{2mA} + \hat{V}_{NN}^{(i,j)} \right) + \sum_{i < j < k} \hat{V}_{3N}^{(i,j,k)}.$$
 (5)

The NN and 3N parts are taken from a next-to-next-to-next-to-leading order (N3LO) chiral nucleon–nucleon interaction, and a next-to-next-to-leading order (N2LO) chiral three-body interaction, respectively. For both IM-SRG and CCEI, we use $\Lambda_{NN}=500\,\text{MeV}$ for the chiral N3LO NN interaction [31,32] and $\Lambda_{3N}=400\,\text{MeV}$ for the chiral N2LO 3N interaction [33], respectively.

To achieve faster model-space convergence in CCEI, the similarity renormalization group transformation has been used to evolve two-body and three-body forces to the lower momentum scale $\lambda_{SRG} = 2.0 \, \text{fm}^{-1}$ (see Ref. [34] for further details). Also, for the coupled-cluster calculations, a

Hartree–Fock basis built from 13 major harmonic oscillator orbitals with frequency $\hbar\Omega=20\,\text{MeV}$ has been used.

We can expand the Hamiltonian for the suitable model space using the valence-cluster expansion [35] given as

$$H_{\text{CCEI}}^A = H_0^{A_{\text{C}}} + H_1^{A_{\text{C}}+1} + H_2^{A_{\text{C}}+2} + \cdots,$$
 (6)

where A is the mass of the nucleus for which we are doing calculations, $H_0^{A_C}$ is the core Hamiltonian, $H_1^{A_C+1}$ is the valence one-body Hamiltonian, and $H_2^{A_C+2}$ is the two-body Hamiltonian. The two-body term is derived from Eq. (6) by using the Okubo–Lee–Suzuki (OLS) similarity transformation [36,37]. After using this unitary transformation the effective Hamiltonian becomes non-Hermitian.

To change the non-Hermitian to Hermitian effective Hamiltonian the metric operator $[S^{\dagger}S] = P_2(1 + \omega^{\dagger}\omega)P_2$ is used, where S is a matrix that diagonalizes the Hamiltonians (see Ref. [38] for further details). After using the metric operator the Hermitian shell model Hamiltonian is then obtained as $[S^{\dagger}S]^{1/2}\hat{H}_{CCEI}^A[S^{\dagger}S]^{-1/2}$. Using IM-SRG targeted for a particular nucleus [39] and CCEI interactions, the shell model results for spectroscopic factors and electromagnetic properties are reported in Refs. [40,41]. In the case of CCEI, the core is fixed to be ¹⁶O and no target normal ordering is carried out.

Recently, L. Huth et al. [22] derived a shell model interaction from chiral effective field theory (CEFT). The valence-space Hamiltonian for the sd shell is constructed as a general operator having two low-energy constants (LECs) at leading order (LO) and seven new LECs at next-to-leading order (NLO), and the LECs of CEFT operators fitted directly to 441 ground- and excited-state energies. For the CEFT interaction they took the expansion in terms of powers of $(Q/\Lambda_b)^{\nu}$ based on Weinberg power counting [42], where Q is a low-momentum scale or pion mass m_{π} and $\Lambda_b \sim 500$ MeV is the chiral-symmetry-breaking scale.

2.2. Beta-decay theory

In beta-decay, the ft value corresponding to GT transition from the initial state i of the parent nucleus to the final state f in the daughter nucleus is expressed as [43]

$$f_A t_{i \to f} = \frac{6177}{[B(GT; i \to f)]},\tag{7}$$

where B(GT) is the Gamow–Teller transition strength, and f_A is the axial vector phase space factor that contains the lepton kinematics. In this work, we have calculated the phase space factor f_A with parameters given by Wilkinson and Macefield [44] together with the correction factors given in Refs. [45,46]. The f_t values are very large, so they are defined in term of "log f_t " values, expressed as $\log f_t = \log_{10}(f_A t_{i \to f})$.

The total half-life $T_{1/2}$ is related to the partial half-life as

$$\frac{1}{T_{1/2}} = \sum_{f} \frac{1}{t_{i \to f}},\tag{8}$$

where f runs over all the possible daughter states that are populated through GT transitions.

The partial half-life is related to the total half-life $T_{1/2}$ of the allowed β^- -decay as

$$t_{i \to f} = \frac{T_{1/2}}{b_r},\tag{9}$$

where b_r is called the branching ratio for the transition with partial half-life $t_{i \to f}$.

The Gamow–Teller strength B(GT) is calculated using the following expression:

$$B(GT; i \to f) = (g_A^{\text{eff}})^2 \frac{1}{2J_i + 1} |\langle f || \sum_k \sigma^k \tau_{\pm}^k ||i\rangle|^2.$$
 (10)

The effective axial-vector coupling constant is calculated from $g_A^{\text{eff}} = qg_A^{\text{free}}$, where $g_A^{\text{free}} = -1.260$, and q is the quenching factor. $|i\rangle$ and $|f\rangle$ are the initial and final state shell-model wave functions, respectively, and τ_{\pm} refers to the isospin operator for the β^{\pm} decay; for the β^{-} -decay we use the convention $\tau_{-}|n\rangle = |p\rangle$. J_i is the initial-state angular momentum.

Following Refs. [5,7,47], we define

$$M(GT) = [(2J_i + 1)B(GT)]^{1/2},$$
(11)

which is independent of the direction of the transitions.

R(GT) values are defined as

$$R(GT) = M(GT)/W, (12)$$

where the total strength W is defined by

$$W = \begin{cases} |g_A/g_V|[(2J_i+1)3|N_i-Z_i|]^{1/2} & \text{for } N_i \neq Z_i, \\ |g_A/g_V|[(2J_f+1)3|N_f-Z_f|]^{1/2} & \text{for } N_i = Z_i. \end{cases}$$
(13)

Here, g_V (= 1.00) is the vector coupling constant; N_i (N_f), Z_i (Z_f) are the neutron and proton numbers of the initial (final) states, respectively; and J_i (J_f) is the angular momentum of the initial (final) state. In the β^- -decay the endpoint energy of the electron E_0 (in units of MeV) is an essential quantity for calculating the phase space factor f_A . E_0 is given by the expression [5]

$$E_0 = (Q + E_i) - E_f, (14)$$

where Q is the β -decay Q value, and E_i and E_f are the excitation energies of the initial and final states. Here, we have taken Q values from the experimental data [3].

3. Results and discussions

In Table 1 we compare calculated and experimental values of the matrix elements M(GT). The calculated values of M(GT) presented here are those with q=1. The β -decay energies (Q), branching ratios (I_{β}) , and $\log ft$ values, as well as the values of W, are given in Table 1. The quenching factors are obtained by chi-squared fitting of the theoretical R(GT) values to the corresponding experimental R(GT) values. The quenching factors as well as the root-mean-square (RMS) deviations for the effective interactions considered here are given in Table 2. The quenching factors change slightly for different effective interactions. Their values are in the range q=0.62–0.77. The value for USDB, $q=0.77\pm0.02$, is consistent with the value q=0.764 obtained for the USDB by the shell model in the sd shell as reported in Ref. [48]. We obtained the RMS deviation values 0.0469, 0.0440, 0.0541, and 0.0356 corresponding to IM-SRG, CCEI, CEFT, and USDB interactions, respectively. We see that the RMS deviations for the ab initio and CEFT interactions are slightly higher than for the USDB interaction. As a result, the points for USDB in Fig. 1 concentrate on the diagonal line.

Table 1. Experimental and theoretical M(GT) matrix elements. I_{β} are the branching ratios. J_n^{π} and T_n^{π} are the spin-parity and isospin of the final states, respectively, where n distinguishes the states with the same J in order of energy. All other quantities are explained in the text. The experimental data were taken from Ref. [1].

	-					-		M(GT)			
$^{A}Z_{i}(J^{\pi})$	$^{A}Z_{f}$	$2J_n^{\pi}, 2T_n^{\pi}$	Q (MeV)	I_{β} (%)	$\log ft(\exp.)$	EXPT	USDB	IM-SRG	CCEI	CEFT	W
$\overline{{}^{19}\text{O}(5/2^+)}$	¹⁹ F	7+,1	0.442	0.0984(30)	3.86(17)	2.262	3.406	3.910	3.640	2.334	9.259
		$5^{+},1$	4.622	45.4(15)	5.38(15)	0.393	0.243	0.256	0.416	0.593	
		$3_{1}^{+},1$	3.266	54.4(12)	4.62(10)	0.939	1.245	1.468	1.556	0.596	
$^{20}{\rm O}(0^+)$	20 F	$2_{1}^{+},2$	2.757	99.97(3)	3.73(6)	1.072	1.104	1.399	1.527	0.887	4.365
		$2^{+}_{2},2$	0.325	0.027(3)	3.64(6)	1.190	1.281	0.989	0.963	0.025	
$^{21}O(5/2^{+})$	^{21}F	$3^{-},3$	6.380	37.2(12)	5.22(2)	0.473	0.464	0.367	0.360	0.223	11.953
$^{22}O(0^{+})$	^{22}F	$2_{1}^{+},4$	4.860	31(5)	4.6(1)	0.394	0.403	0.509	0.473	0.573	5.346
		$2^{+}_{2},4$	3.920	68(8)	3.8(1)	0.989	1.234	0.066	1.686	0.675	
$^{24}O(0^{+})$	²⁴ F	$2^{+},6$	9.700	40(4)	4.3(1)	0.556	0.990	0.782	0.857	1.024	6.173
$^{20}\text{F}(2^+)$	²⁰ Ne	$4^{+},0$	5.390	99.99(8)	4.97(11)	0.575	0.687	0.679	0.651	0.694	6.901
$^{21}\text{F}(5/2^+)$	²¹ Ne	$7^{+},1$	3.938	16.1(10)	4.72(3)	0.840	0.959	1.046	1.123	0.655	9.259
		$5^{+},1$	5.333	74.1(22)	4.65(1)	0.911	0.982	1.143	1.338	0.858	
		$3^{+},1$	5.684	9.6(30)	5.67(16)	0.281	0.371	0.421	0.515	0.360	
$^{22}\text{F}(4^+)$	²² Ne	$10^{+},2$	3.480	8.7(4)	4.70(2)	1.053	1.250	1.372	1.362	0.940	13.094
		$8_{1}^{+},2$	7.461	3.1(6)	6.7(1)	0.105	0.106	0.156	0.099	0.066	
		$8^{+}_{2},2$	5.500	53.9(6)	4.79(1)	0.950	1.174	1.173	1.365	1.048	
		$8^{\frac{1}{4}}_{3},2$	4.670	7.0(3)	5.34(2)	0.504	0.406	0.107	0.287	0.706	
		$8_{4}^{+},2$	3.477	2.45(22)	5.30(4)	0.528	0.733	0.939	1.280	0.357	
		$6^{+},2$	5.177	16.4(7)	5.26(2)	0.553	0.678	0.649	0.660	0.382	
$^{23}F(5/2^+)$	²³ Ne	$5_{1}^{+},3$	8.480	30(8)	5.72(16)	0.266	0.377	0.333	0.321	0.428	11.953
(, ,		$3^{+}_{1},3$	6.660	10.9(19)	5.66(11)	0.285	0.262	0.256	0.305		
		$3^{+}_{2},3$	5.050	15.2(12)	4.96(8)	0.637	0.866	1.028	1.171		
		$3^{2}_{3},3$	4.650	25(4)	4.58(12)	0.987	0.200	0.260	0.272		
$^{26}\text{F}(1^+)$	²⁶ Ne	$4^{+},6$	16.170	36(7)	4.6(1)	0.682	1.145	1.079	1.065	0.858	10.691
` '		$0^{+},6$	18.900	36.5(60)	4.9(1)	0.483	0.733	0.756	0.714	0.719	
23 Ne(5/2 ⁺)	²³ Na	$5^{+},1$	3.950	32.0(13)	5.38(2)	0.393	0.372	0.392	0.753	0.656	9.259
` ' '		$3_{1}^{+},1$	4.383	66.9(13)	5.27(1)	0.446	0.355	0.585	0.888	0.516	
$^{24}\text{Ne}(0^+)$	²⁴ Na	$2^{+}_{1},2$	1.994	92.1(2)	4.35(1)	0.525	0.571	0.442	0.664	0.053	4.365
` '		$2^{+}_{2},2$	1.120	7.9(2)	4.39(2)	0.502	0.542	0.848	1.068	0.986	
25 Ne $(1/2^+)$	²⁵ Na	$3^{\frac{1}{4}}_{1},3$	7.160	76.6(20)	4.41(2)	0.693	0.751	0.751	0.697	0.604	6.901
. , ,		$1_{1}^{+},3$	6.180	19.5(20)	4.70(6)	0.496	0.597	0.419	0.547	0.724	
		$1^{+}_{2},3$	2.960	0.53(15)	4.82(16)	0.432	0.595	0.713	1.037	0.657	
$^{26}\text{Ne}(0^+)$	²⁶ Na	$2^{\frac{7}{4}},4$	7.258	91.6(2)	3.87(6)	0.913	1.110	1.302	1.247	1.036	5.346
		$2^{+}_{2},4$	5.829	4.2(4)	4.8(1)	0.313	0.669	0.022	0.309	0.666	
		$2^{2}_{3},4$	4.619	1.9(4)	4.7(1)	0.351	0.616	0.547	0.818	0.892	
27 Ne $(3/2^{+})$	²⁷ Na	$5^{+},5$	12.590	59.5(30)	4.40(4)		1.229	1.042	1.059	1.258	11.548
$^{28}\text{Ne}(0^+)$	²⁸ Na		12.280	55(5)	4.2(1)		1.185	1.104			6.173
. ,							0.816	0.734	0.352		
		$2^{+}_{2},6$	10.350	1./(4)	5.3(1)	0.170	0.010	0.754	0.552	0.077	
		$2^{+}_{2},6$ $2^{+}_{3},6$	10.350 10.160	1.7(4) 20.1(12)	5.3(1) 4.2(1)		0.341	0.734	0.677		
		$2_{3}^{+},6$	10.350 10.160 9.570	20.1(12) 8.5(6)	4.2(1) 4.5(1)	0.624				0.333	
²⁴ Na(4 ⁺)	²⁴ Mg	$2_{3}^{+},6$ $2_{4}^{+},6$	10.160	20.1(12)	4.2(1)	0.624 0.442	0.341	0.484	0.677 1.293	0.333	9.259
²⁴ Na(4 ⁺) ²⁵ Na(5/2 ⁺)		2 ⁺ ,6 2 ⁺ ,6 8 ⁺ ,0	10.160 9.570	20.1(12) 8.5(6)	4.2(1) 4.5(1)	0.624 0.442 0.208	0.341 0.471	0.484 0.394	0.677 1.293	0.333 0.189 0.355	9.259 9.259
		2 ₃ ⁺ ,6 2 ₄ ⁺ ,6 8 ⁺ ,0	10.160 9.570 1.392	20.1(12) 8.5(6) 99.855(5)	4.2(1) 4.5(1) 6.11(1)	0.624 0.442 0.208	0.341 0.471 0.338	0.484 0.394 0.125	0.677 1.293 0.065	0.333 0.189 0.355 0.471	
		2 ⁺ ₃ ,6 2 ⁺ ₄ ,6 8 ⁺ ,0 7 ⁺ ,1 5 ⁺ ₁ ,1	10.160 9.570 1.392 2.223	20.1(12) 8.5(6) 99.855(5) 9.48(14)	4.2(1) 4.5(1) 6.11(1) 5.03	0.624 0.442 0.208 0.588	0.341 0.471 0.338 0.642	0.484 0.394 0.125 0.629	0.677 1.293 0.065 0.577	0.333 0.189 0.355 0.471 0.685	
	²⁵ Mg	$2_{3}^{+},6$ $2_{4}^{+},6$ $8^{+},0$ $7^{+},1$ $5_{1}^{+},1$ $3_{1}^{+},1$ $3_{2}^{+},1$	10.160 9.570 1.392 2.223 3.835	20.1(12) 8.5(6) 99.855(5) 9.48(14) 62.5(20)	4.2(1) 4.5(1) 6.11(1) 5.03 5.26	0.624 0.442 0.208 0.588 0.451	0.341 0.471 0.338 0.642 0.558	0.484 0.394 0.125 0.629 0.636	0.677 1.293 0.065 0.577 1.169	0.333 0.189 0.355 0.471 0.685 0.633	
²⁵ Na(5/2 ⁺)	²⁵ Mg	$2_{3}^{+},6$ $2_{4}^{+},6$ $8^{+},0$ $7^{+},1$ $5_{1}^{+},1$ $3_{1}^{+},1$ $3_{2}^{+},1$	10.160 9.570 1.392 2.223 3.835 2.860	20.1(12) 8.5(6) 99.855(5) 9.48(14) 62.5(20) 27.46(22) 0.247(4)	4.2(1) 4.5(1) 6.11(1) 5.03 5.26 5.04	0.624 0.442 0.208 0.588 0.451 0.581 0.457	0.341 0.471 0.338 0.642 0.558 0.708	0.484 0.394 0.125 0.629 0.636 0.842	0.677 1.293 0.065 0.577 1.169 0.748 1.010	0.333 0.189 0.355 0.471 0.685 0.633 0.910	9.259
		$2_{3}^{+},6$ $2_{4}^{+},6$ $8^{+},0$ $7^{+},1$ $5_{1}^{+},1$ $3_{1}^{+},1$ $3_{2}^{+},1$	10.160 9.570 1.392 2.223 3.835 2.860 1.033	20.1(12) 8.5(6) 99.855(5) 9.48(14) 62.5(20) 27.46(22)	4.2(1) 4.5(1) 6.11(1) 5.03 5.26 5.04 5.25	0.624 0.442 0.208 0.588 0.451 0.581 0.457 0.242	0.341 0.471 0.338 0.642 0.558 0.708 0.683	0.484 0.394 0.125 0.629 0.636 0.842 0.712	0.677 1.293 0.065 0.577 1.169 0.748 1.010	0.333 0.189 0.355 0.471 0.685 0.633 0.910 0.580	
²⁵ Na(5/2 ⁺)	²⁵ Mg	$2_{3}^{+}, 6$ $2_{4}^{+}, 6$ $8^{+}, 0$ $7^{+}, 1$ $5_{1}^{+}, 1$ $3_{1}^{+}, 1$ $3_{2}^{+}, 1$ $6_{1}^{+}, 2$	10.160 9.570 1.392 2.223 3.835 2.860 1.033 5.413	20.1(12) 8.5(6) 99.855(5) 9.48(14) 62.5(20) 27.46(22) 0.247(4) 1.31(4)	4.2(1) 4.5(1) 6.11(1) 5.03 5.26 5.04 5.25 5.87(1)	0.624 0.442 0.208 0.588 0.451 0.581 0.457 0.242	0.341 0.471 0.338 0.642 0.558 0.708 0.683 0.226 0.714	0.484 0.394 0.125 0.629 0.636 0.842 0.712 0.377	0.677 1.293 0.065 0.577 1.169 0.748 1.010 0.316	0.333 0.189 0.355 0.471 0.685 0.633 0.910 0.580 0.504	9.259

Table 1. (Continued.)

								M(GT)			
$^{A}Z_{i}(J^{\pi})$	$^{A}Z_{f}$	$2J_n^{\pi}, 2T_n^{\pi}$	Q (MeV)	I_{β} (%)	$\log ft(\exp.)$	EXPT	USDB		CCEI	CEFT	W
		$4_{2}^{+},2$	6.416	0.05(4)	7.60(4)	0.033	0.129	0.404		0.047	
		$4_3^+,2$	5.022	1.65(3)	5.62(1)	0.322	0.411	1.037		0.552	
		$4_{4}^{+},2$	4.519	2.738(19)		0.493	0.558	0.149		0.648	
27 Na(5/2 ⁺)	27 Mg	$5_1^+,3$	7.310	11.3(7)	4.99(3)	0.616	0.602	0.406		0.650	11.953
		$3^{+},3$	8.030	85.8(11)	4.30(15)	1.363	1.747	1.683		1.509	
28 Na(1 ⁺)	28 Mg	$4_1^+,4$	12.556	11(6)	5.1(2)	0.384	0.294	0.438		0.245	9.259
		$2_{1}^{+},4$	9.469	3.2(4)	5.1(1)	0.384	0.536	0.583		0.925	
		$0_1^+,4$	14.030	60(5)	4.6(1)	0.682	0.840	0.702		0.882	
		$0_{2}^{+},4$	10.168	20.1(19)	4.42(1)	0.839	1.116	1.174		0.787	
29 Na(3/2 ⁺)	29 Mg	$3^{+},5$	13.272	24(8)	5.06(15)	0.464	0.786	0.737			11.548
30 Na(2 ⁺)	30 Mg	$4_1^+,6$	15.790	9.5(11)	5.86(6)	0.206	0.408	0.451			13.803
27 Mg(1/2 ⁺)	^{27}Al	$3^{+},1$	1.596	29.06(9)	4.934(16)	0.381	0.450	0.373		0.468	5.346
		$1^{+},1$	1.766	70.94(9)	4.73(10)	0.480	0.597	0.178		0.766	
28 Mg(0 ⁺)	28 A1	$2_1^+,2$	0.459	94.8(10)	4.45(9)	0.468	0.624	0.379		0.581	4.365
		$2_{2}^{+},2$	0.211	4.9(10)	4.57(9)	0.408	0.495	0.454		1.029	
$^{29}Mg(3/2^+)$	²⁹ Al	$5_1^+,3$	7.613	27(8)	5.32(14)	0.344	0.579	0.403		0.829	9.760
		$5_{2}^{+},3$	4.551	6.0(16)	4.93(13)	0.539	1.064	1.194		1.193	
		$5_3^+,3$	4.428	28(5)	4.21(9)	1.234	1.098	0.367		0.954	
		$3_1^+,3$	5.389	21(6)	4.73(13)	0.678	0.658	0.341		0.187	
		$3_{2}^{+},3$	4.747	7.8(15)	4.90(10)	0.558	0.669	0.806		0.833	
		$1_{1}^{+},3$	6.215	7(3)	5.49(19)	0.283	0.283	0.198		0.067	
		$1_{2}^{+},3$	4.180	3.0(9)	5.06(14)	0.464	0.710	0.383		0.380	
$^{30}{ m Mg}(0^+)$	30 A1	$2_{1}^{+},4$	6.274	68(20)	3.96(13)	0.823	1.203	1.167		1.337	5.346
		$2^{+}_{2},4$	4.549	7(1)	4.30(7)	0.556	0.870	0.783		0.800	
$^{32}{ m Mg}(0^+)$	³² A1	$2_1^+,6$	10.150	55	4.4	0.496	1.596	1.531		1.450	6.173
		$2^{+}_{2},6$	7.380	24.6(8)	4.1	0.700	0.303	0.385		0.190	
••	• 0	$2_3^+,6$	6.950	10.7(10)	4.4	0.496	0.013	0.072		0.025	
$^{28}\text{Al}(3^+)$	²⁸ Si	$4^{+},0$	2.863	99.99(1)	4.87(4)	0.764	0.945	0.353		0.920	8.166
$^{29}\text{Al}(5/2^+)$	²⁹ Si	$3_{1}^{+},1$	2.406	89.9(3)	5.05(5)	0.575	0.924	0.237	0.388		9.259
•	• •	$3_{2}^{+},1$	1.253	6.3(2)	5.03(15)	0.591	0.589	0.591		1.059	
30 Al(3 ⁺)	30 Si	$6_1^+,2$	3.730	6.6(2)	4.985(17)	0.669	1.001	0.673			11.548
		$6_{2}^{+},2$	3.329	2.6(2)	5.17(4)	0.541	0.657	0.229		0.167	
		$4_1^+,2$	6.326	17.1(9)	5.619(25)	0.322	0.362	0.379		0.157	
		$4_{2}^{+},2$	5.063	67.3(11)	4.578(12)	1.069	1.417	1.192		1.189	
22	22	$4_{3}^{+},2$	3.751	5.7(2)	5.06(19)		0.762	0.067	0.476		
$^{32}Al(1^+)$	³² Si	$4_{1}^{+},4$	11.080	4.7(13)	5.29(13)		0.181	0.122			9.259
		$4_{2}^{+},4$	8.790	3.0(8)	5.00(12)		0.590	0.754		0.625	
		$0_1^+,4$	13.020	85(5)	4.36(3)	0.899	1.093	0.846		1.157	
	22	$0_2^+,4$	8.040	4.3(11)	4.66(12)	0.637	1.229	1.336		0.938	
33 Al $(5/2^+)$	33Si	3+,5	11.960	88(2)	4.3	1.363	2.225	1.966			14.143
$^{31}\text{Si}(3/2^+)$	³¹ P	1+,1	1.491	99.94(7)	5.525(8)		0.318	0.076		0.389	7.560
$^{32}\text{Si}(0^{+})$	^{32}P	2+,2	0.227	100	8.21(6)	0.006		0.136		0.384	4.365
$^{33}\text{Si}(3/2^+)$	³³ P	1+,3	5.845	93.7(7)	4.96(17)	0.520	0.264	0.394		0.329	9.760
$^{34}\text{Si}(0^+)$	³⁴ P	2+,4	2.984	100	≥3.3	1.759	0.639	0.372		0.232	5.346
$^{32}P(1^+)$	^{32}S	$0^{+},0$	1.710	100	7.90(2)	0.015	0.038	0.140		0.352	5.346
$^{33}P(1/2^+)$	^{33}S	3+,1	0.248	100	5.022(7)	0.343	0.295	0.025		0.337	5.346
$^{34}P(1^+)$	^{34}S	$4_1^+,2$	3.255	14.8(20)	4.93(6)	0.467	0.742	0.533		0.837	7.560
		$4_{2}^{+},2$	1.268	0.31(6)	4.88(9)	0.494		0.313		0.229	
		$0_1^+,2$	5.383	84.8(21)	5.159(12)	0.358	0.480	0.180	1.545	0.269	

Table 2. Quenching factor for the different effective interactions.

q	RMS deviations				
0.77 ± 0.02	0.0356				
0.75 ± 0.03	0.0469				
0.62 ± 0.03	0.0440				
0.73 ± 0.04	0.0541				
	0.77 ± 0.02 0.75 ± 0.03 0.62 ± 0.03				

We have plotted the experimental R(GT) values with respect to the theoretical R(GT) values for the sd-shell nuclei in Fig. 1. In this figure there are some isolated points, e.g. around $R(GT)_{\rm Expt}=0.3$. This is because the experimental M(GT) value (experimental value of $\log ft \geq 3.3$) corresponding to the transition $^{34}{\rm Si}(0^+) \rightarrow ^{34}{\rm P}(1^+)$ is large compared to the theoretical value. This deviation is due to experimental uncertainty. When the calculated and experimental R(GT) values are the same, then these points will be on the diagonal line. The different sources of renormalization [49–53] affecting the values of g_A depend on (i) missing configurations outside the sd-shell, (ii) non-nucleonic degrees of freedom such as Δ_{33} resonance, and (iii) many-body operators induced by unitary transformations in the ab initio method. In the shell model we need an effective value of g_A to reproduce the experimental results. In our calculation corresponding to $|g_A^{\rm free}|=1.26$, we have obtained values of $|g_A^{\rm eff}|$ of 0.97, 0.95, and 0.92 for USDB, IM-SRG, and CEFT interactions, respectively. These values are close to unity; however, the CCEI interaction gives 0.78, far from unity. For further calculations we have used the effective value of g_A corresponding to different interactions.

In Fig. 2 we show the distribution of calculated $\log ft$ values with the experimental data for some β^- -decays nuclei for which experimental $\log ft$ values are also available for excited states. In the case of 21 F, although the results of the ab initio interactions for the excitation energy of the excited $3/2^+$, $5/2^+$, and $7/2^+$ states differ slightly from the experimental data, all the interactions give calculated $\log ft$ values close to the experimental data. For 28 Ne, the calculated $\log ft$ values with CCEI are better in comparison to other interactions, although CCEI and IM-SRG interactions are not able to correctly reproduce energy levels in comparison to USDB and CEFT interactions. The calculated value for the excitation energy of the 2_1^+ state is in good agreement for all the interactions for 28 Na. For this nucleus all four interactions give reasonable results for $\log ft$.

In Fig. 3 we compare the theoretical and experimental β -decay half-lives of sd=shell nuclei. Here, we make some general comments on the half-lives.

- (1) For O and F isotopes, the calculated half-lives are in fair agreement with the experimental values within a factor of 2.1–2.2, except for ²²O obtained with IM-SRG.
- (2) The discrepancy between calculated and experimental half-life becomes large (a) when the discrepancy between the calculated and experimental B(GT) is large, or (b) when the transition with the dominant branching ratio is different between calculation and experiment, or (c) when the Q value for the transition is small and the difference between the calculated and experimental excitation energies is large enough to lead to a substantial change of the phase space factor for the transition. In the case of 22 O with IM-SRG, a large discrepancy comes from the combined effects of (a) and (b). Nuclei in the island of inversion such as 32 Mg cannot be well described for both the ab initio and phenomenological interactions due to reason (a). 28 Mg discussed above corresponds to case (c).

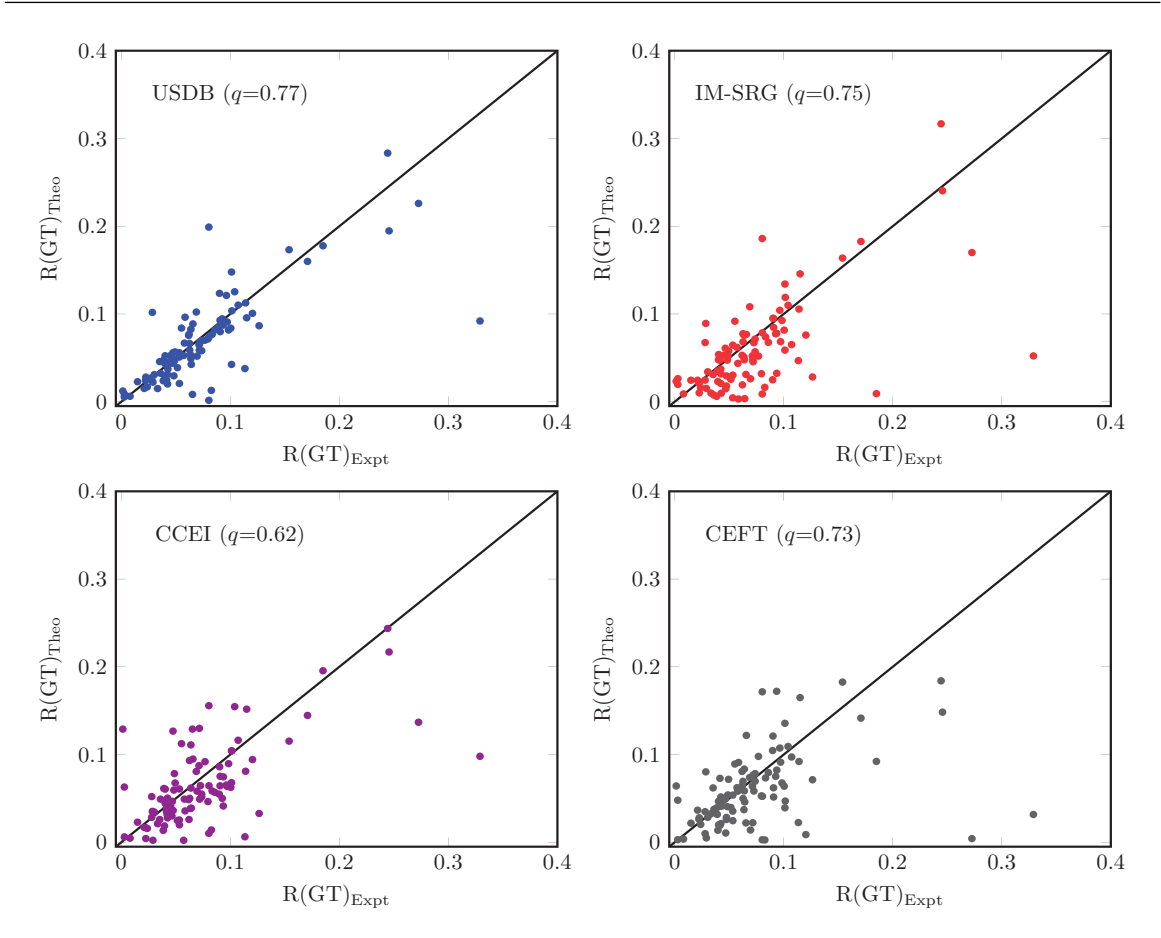


Fig. 1. Comparison of the experimental values of the matrix elements R(GT) with the theoretical ones obtained for the different effective interactions. Each transition is indicated by a point. The experimental and theoretical values are given by the horizontal and vertical coordinates, respectively. When the calculated and experimental R(GT) values are the same, these points will be on the diagonal line.

(3) For isotopes with Z=10-13 (Z=14,15), there are one or two (or more) cases for each Z in which the calculated half-lives differ from the experimental ones by a factor of more than 3 due to reasons (a), (b), or (c) in the case of IM-SRG and CCEI. In general, the calculated half-life results for O, F, Ne, Na, Mg, and Al are in reasonable agreement with the experimental data. The results for P isotopes show deviation from the experimental data. This might be due to missing the pf orbitals in our calculations.

The phase space factor is estimated to be roughly proportional to Q^5 . For example, in the case of the $^{28}\text{Mg}(0^+) \rightarrow ^{28}\text{Al}(1^+)$ transition, the excitation energies for the 1_1^+ state of ^{28}Al obtained for the interactions are smaller than the experimental one, $E_x = 1.373 \,\text{MeV}$, by 0.175, 0.571, 0.251, and 0.018 MeV for USDB, IM-SRG, CCEI, and CEFT, respectively, which leads to an enhancement of the phase space factor by nearly 10 times for IM-SRG. Though the difference of the B(GT) values is within the range of a factor of about 3, a large difference in the phase space factors leads to a larger difference in the half-lives.

4. Summary and conclusions

We have performed shell model calculations using ab initio approaches along with interactions based on chiral effective field theory and phenomenological USDB interaction, and evaluated B(GT), $\log ft$

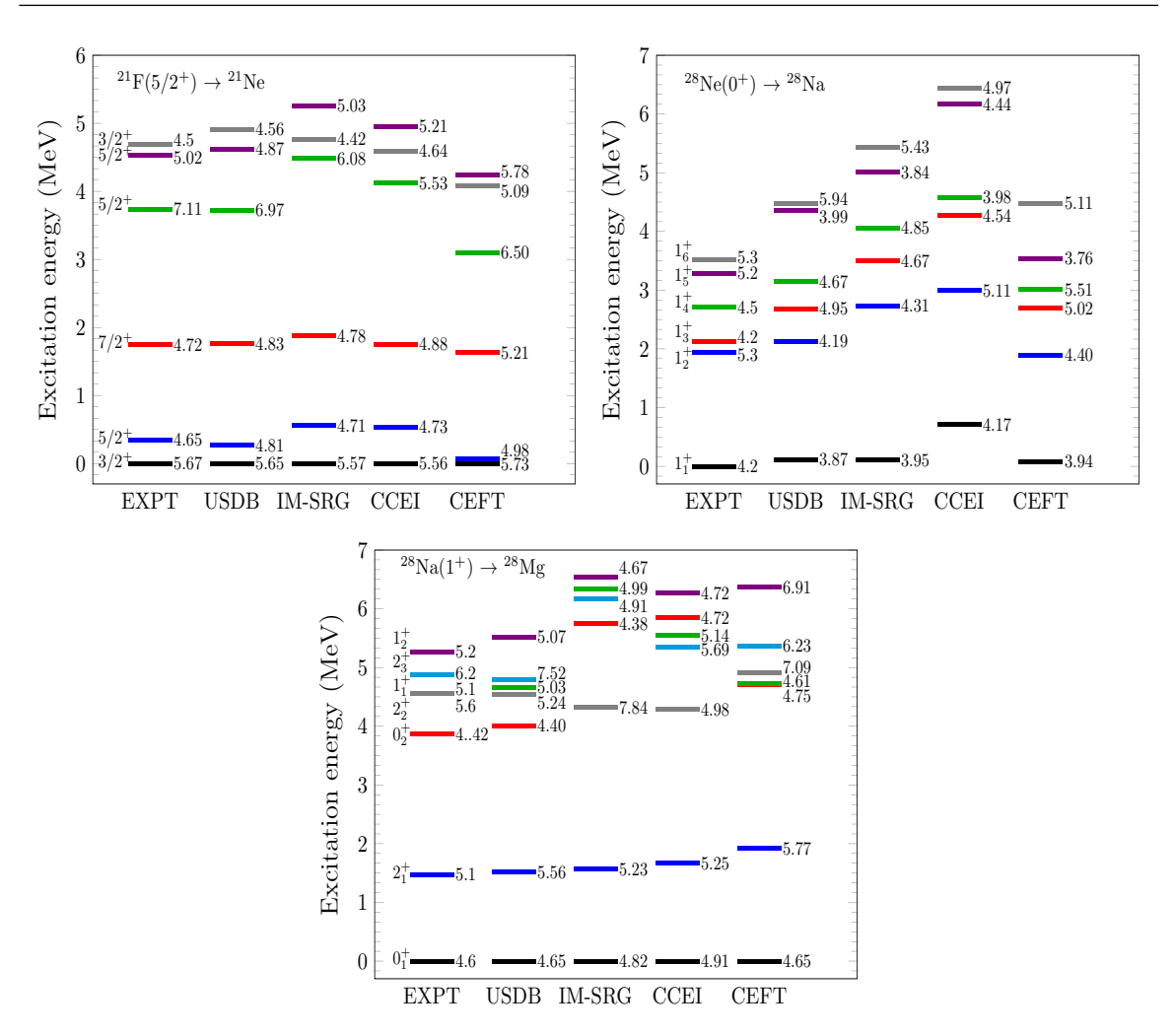


Fig. 2. Comparison of experimental and theoretical (with different interactions) distributions of $\log ft$ values for the β^- -decay for 21 F, 28 Ne, and 28 Na.

values, and half-lives for the sd-shell nuclei. Since these ab initio effective interactions are developed using state-of-the-art approaches, our aim was to test the predicting power of these interactions for β^- -decay properties.

We find that all the ab initio interactions, as well as the fitted interaction based on chiral effective theory, considered here need quenching of the *GT* strengths by as much as 44%–62% compared with the phenomenological USDB interaction.

The quenching factor can be attributed to (i) configurations outside the *sd* shell, (ii) the induced effective Gamow–Teller operator due to the unitary transformation in the ab initio approach, and (iii) the intrinsic two-body Gamow–Teller operator connected with the 3N interaction.

An effective value needs to be used for the weak axial coupling constant g_A in the shell model calculation. In our calculation corresponding to $|g_A^{\text{free}}| = 1.26$, we have obtained the value of $|g_A^{\text{eff}}|$ by chi-squared fitting as 0.95, 0.78, and 0.92 for IM-SRG, CCEI, and CEFT interactions, respectively, while it has been obtained as 0.97 for USDB. We have also obtained the RMS deviation values 0.0469, 0.0440, 0.0541, and 0.0356 corresponding to IM-SRG, CCEI, CEFT, and USDB interactions, respectively. The RMS deviations for the ab initio and CEFT interactions are slightly enhanced compared with the USDB interaction. Within the present framework of using the one-body operator

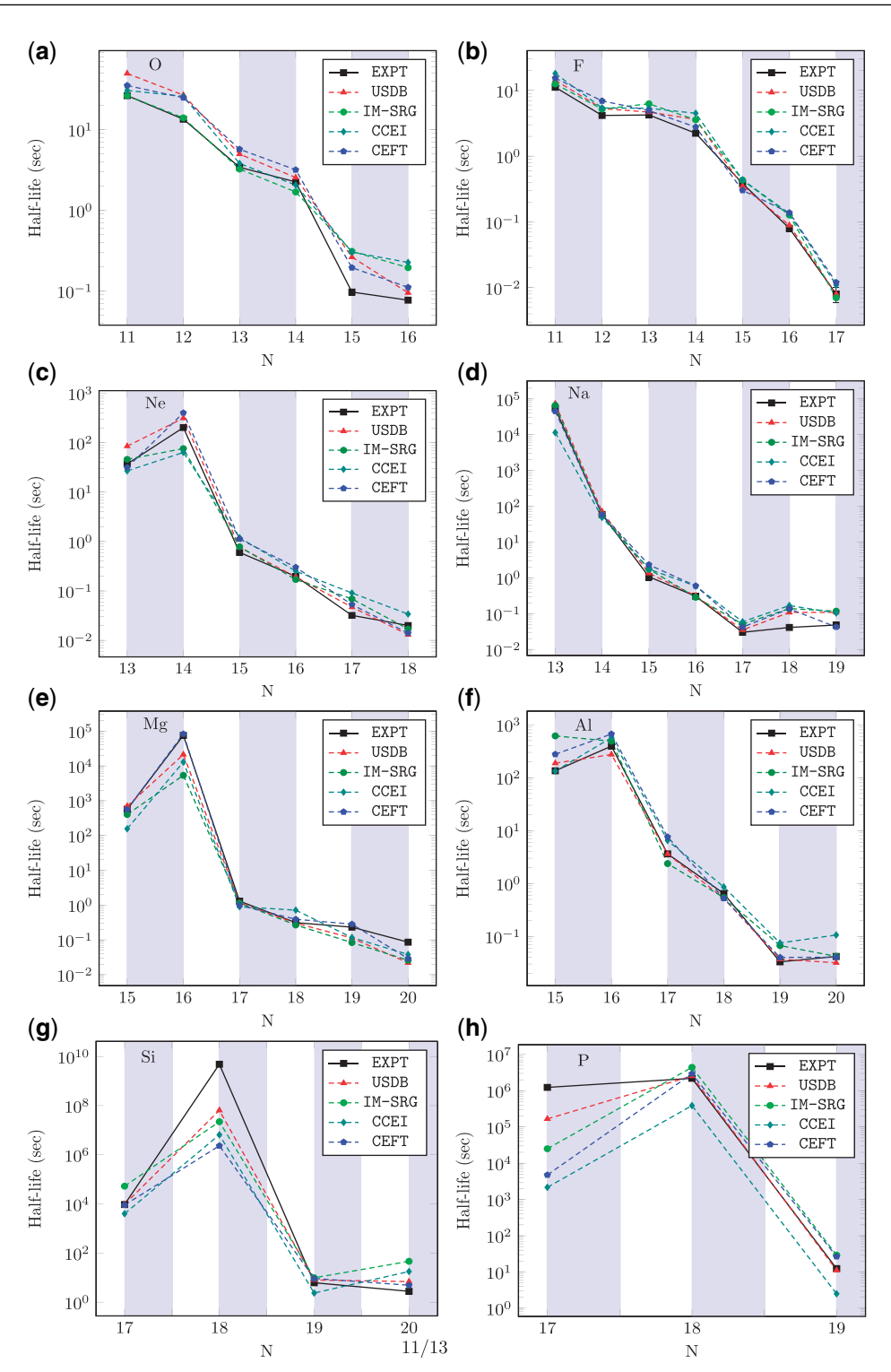


Fig. 3. Plot of half-lives versus neutron numbers of sd-shell nuclei.

with effective g_A , the ab initio IM-SRG interaction can be considered as the most favorable since both the quenching factor and the RMS deviation are close to those of the phenomenological USDB. The calculated half-life results for O, F, Ne, Na, Mg, and Al are in reasonable agreement

with the experimental data for the ab initio interactions. However, it is rather hard to reproduce

both the transition strength and energy levels in nuclei such as ²⁸Ne and ³²Mg in the island of inversion.

In case of the ab initio approaches, IM-SRG and CCEI, both the intrinsic and induced two-body operators can be constructed in principle, and the contributions from configurations outside the *sd* shell can be reliably constrained. The quenching factors can become closer to unity with the inclusion of the two-body operators [54]. It would also be interesting to expand the configuration space outside the *sd* shell so that we can treat nuclei in the island of inversion more appropriately.

Acknowledgements

AK acknowledges financial support from MHRD for his Ph.D. thesis work. PCS would like to thank Prof. Gabriel Martínez Pinedo and Prof. Thomas Neff for useful discussion on this work. TS would like to acknowledge support from Japan Society for the Promotion of Science (JSPS) KAKENHI under Grant No. 15K05090.

References

- [1] National Nuclear Data Center, *ENSDF database* (NNDC, Upton, NY, 2020). (Available at: http://www.nndc.bnl.gov/ensdf/, date last accessed February 24, 2020).
- [2] G. Audi, F. G. Kondev, M. Wang, W. J. Huang, and S. Naimi, Chin. Phys. C 41, 030001 (2017).
- [3] M. Wang, G. Audi, F. G. Kondev, W. J. Huang, S. Naimi, and X. Xu, Chin. Phys. C 41, 030003 (2017).
- [4] B. H. Wildenthal, M. S. Curtin, and B. A. Brown, Phys. Rev. C 28, 1343 (1983).
- [5] B. A. Brown and B. H. Wildenthal, At. Data Nucl. Data Tables 33, 347 (1985).
- [6] D. H. Wilkinson, Nucl. Phys. A 209, 470 (1973).
- [7] W.-T. Chou, E. K. Warburton, and B. A. Brown, Phys. Rev. C 47, 163 (1993).
- [8] H. Li and Z. Ren, J. Phys. G: Nucl. Part. Phys. 40, 105110 (2013).
- [9] J. Menéndez, D. Gazit, and A. Schwenk, Phys. Rev. Lett. 107, 062501 (2011).
- [10] J. Suhonen, From Nucleons to Nucleus: Concepts of Microscopic Nuclear Theory (Springer, Berlin, 2007).
- [11] J. Engel, M. Bender, J. Dobaczewski, W. Nazarewicz, and R. Surman, Phys. Rev. C 60, 014302 (1999).
- [12] P. Möller, J. R. Nix, and K.-L. Kratz, At. Data Nucl. Data Tables 66, 131 (1997).
- [13] P. Möller, B. Pfeiffer, and K.-L. Kratz, Phys. Rev. C 67, 055802 (2003).
- [14] P. Sarriguren, A. Algora, and G. Kiss, Phys. Rev. C 98, 024311 (2018).
- [15] T. Marketin, L. Huther, and G. Martínez-Pinedo, Phys. Rev. C 93, 025805 (2016).
- [16] D. S. Ahn et al., Phys. Rev. Lett. 123, 212501 (2019).
- [17] A. Saxena, P. C. Srivastava, and T. Suzuki, Phys. Rev. C 97, 024310 (2018).
- [18] K. Tsukiyama, S. K. Bogner, and A. Schwenk, Phys. Rev. Lett. 106, 222502 (2011).
- [19] S. R. Stroberg, H. Hergert, J. D. Holt, S. K. Bogner, and A. Schwenk, Phys. Rev. C 93, 051301(R) (2016).
- [20] G. R. Jansen, J. Engel, G. Hagen, P. Navratil, and A. Signoracci, Phys. Rev. Lett. 113, 142502 (2014).
- [21] G. R. Jansen, M. D. Schuster, A. Signoracci, G. Hagen, and P. Navrátil, Phys. Rev. C **94**, 011301(R) (2016).
- [22] L. Huth, V. Durant, J. Simonis, and A. Schwenk, Phys. Rev. C 98, 044301 (2018).
- [23] B. Alex Brown and W. A. Richter, Phys. Rev. C 74, 034315 (2006).
- [24] B. A. Brown and W. D. M. Rae, Nucl. Data Sheets 120, 115 (2014).
- [25] S. D. Głazek and K. G. Wilson, Phys. Rev. D 48, 5863 (1993).
- [26] F. Wegner, Ann. Phys. (Leipzig) 3, 77 (1994).
- [27] S. K. Bogner, H. Hergert, J. D. Holt, A. Schwenk, S. Binder, A. Calci, J. Langhammer, and R. Roth, Phys. Rev. Lett. 113, 142501 (2014).
- [28] H. Hergert, S. K. Bogner, T. D. Morris, A. Schwenk, and K. Tsukiyama, Phys. Rep. 621, 165 (2016).
- [29] H. Hergert, Phys. Scr. 92, 023002 (2017).
- [30] H. Hergert, S. K. Bogner, J. G. Lietz, T. D. Morris, S. J. Novario, N. M. Parzuchowski, and F. Yuan, In-medium similarity renormalization group approach to the nuclear many-body problem, in *An Advanced Course in Computational Nuclear Physics: Bridging the Scales from Quarks to Neutron Stars*, eds. M. Hjorth-Jensen, M. P. Lombardo, and U. van Kolck (Springer, Berlin, 2017), Chap. 10.

- [31] D. R. Entem and R. Machleidt, Phys. Rev. C 68, 041001(R) (2003).
- [32] R. Machleidt and D. R. Entem, Phys. Rep. 503, 1 (2011).
- [33] P. Navrátil, Few Body Syst. 41, 117 (2007).
- [34] E. D. Jurgenson, P. Navrátil, and R. J. Furnstahl, Phys. Rev. Lett. 103, 082501 (2009).
- [35] A. F. Lisetskiy, B. R. Barrett, M. K. G. Kruse, P. Navratil, I. Stetcu, and J. P. Vary, Phys. Rev. C 78, 044302 (2008).
- [36] S. Ôkubo, Prog. Theor. Phys. 12, 603 (1954).
- [37] K. Suzuki, Prog. Theor. Phys. 68, 246 (1982).
- [38] P. Navrátil and B. R. Barrett, Phys. Rev. C 54, 2986 (1996).
- [39] S. R. Stroberg, A. Calci, H. Hergert, J. D. Holt, S. K. Bogner, R. Roth, and A. Schwenk, Phys. Rev. Lett. 118, 032502 (2017).
- [40] P. C. Srivastava and V. Kumar, Phys. Rev. C 94, 064306 (2016).
- [41] A. Saxena and P. C. Srivastava, Phys. Rev. C 96, 024316 (2017).
- [42] S. Weinberg, Nucl. Phys. B **363**, 3 (1991).
- [43] A. Piechaczek et al., Nucl. Phys. A 584, 509 (1995).
- [44] D. H. Wilkinson and B. E. F. Macefield, Nucl. Phys. A 232, 58 (1974).
- [45] A. Sirlin and R. Zucchini, Phys. Rev. Lett. 57, 1994 (1986).
- [46] D. H. Wilkinson, A. Gallmann, and D. E. Alburger, Phys. Rev. C 18, 401 (1978).
- [47] G. Martínez-Pinedo, A. Poves, E. Caurier and A. P. Zuker, Phys. Rev. C 53, R2602(R) (1996).
- [48] W. A. Richter, S. Mkhize, and B. Alex Brown, Phys. Rev. C 78, 064302 (2008).
- [49] J. T. Suhonen, Fron. Phys. 5, 1 (2017).
- [50] T. Siiskonen, M. Hjorth-Jensen, and J. Suhonen, Phys. Rev. C 63, 055501 (2001).
- [51] L. Coraggio, L. De Angelis, T. Fukui, A. Gargano, and N. Itaco, Phys. Rev. C 95, 064324 (2017).
- [52] A. Arima, K. Shimizu, W. Bentz, and H. Hyuga, Adv. Nucl. Phys. 18, 1 (1987).
- [53] I. S. Towner, Phys. Rep. 155, 263 (1987).
- [54] P. Gysbers et al., Nature Physics 15, 428 (2019).